

The effects of waves and morphology on mass transfer within branched reef corals

Matthew A. Reidenbach,¹ Jeffrey R. Koseff, Stephen G. Monismith, and Jonah V. Steinbuck

Environmental Fluid Mechanics Laboratory, Stanford University, Stanford, California 94305-4020

Amatzia Genin

The Interuniversity for Marine Sciences in Eilat and Department of Evolution, Systematics, and Ecology, The Hebrew University of Jerusalem, P.O. Box 469, Eilat 88103, Israel

Abstract

Rates of mass transfer in coral reefs are governed both by the physical flow environment and the morphology of the coral. Laboratory experiments were conducted to estimate mass transfer in unidirectional and oscillatory flows by measuring the rate of dissolution of gypsum cylinders (clods) placed within the branching structure of three morphologically distinct coral species. Unidirectional flows were varied between 2.9 and 14.1 cm s⁻¹ and, as expected, mass transfer rates increased with increasing flow and a more open branch spacing. Depending on morphology and flow, mass transfer rates within the interior of the branching structure were 50 to 75% of that measured outside the coral in free-stream conditions. Oscillatory conditions showed relative mass transfer rates 1.6 to 2.9 times greater than equivalent unidirectional currents. This ratio increased with increasing wave frequency, likely due to the corresponding decrease in the diffusive boundary layer thickness. The ratio also increased with a greater compactness in branch spacing, with mass transfer rates within the coral structure up to 130% of free-stream conditions. We used planar laser-induced fluorescence imaging to study the instantaneous structure of mass advection through the coral. Oscillatory flow acts as a dominant forcing mechanism to generate water motion within the coral structure at levels not attainable with comparable unidirectional currents.

Coral reefs exist under a wide range of physical environments and flow conditions, from high-energy environments where they are exposed to wave action as well as wave breaking, to low-energy environments where they are exposed to weak currents driven primarily by wind or tides (e.g., Hamner and Wolanski 1988; Kench 1998). Given this variety of physical environments, it is not surprising that studies have shown a link between variations in flow and habitat to coral growth patterns and morphologic zonation (Graus and Macintyre 1989; Sebens and Done 1992). Changes in growth form can occur in response to flow exposure (Lesser et al. 1994), with transformations from compact branching structures under exposed conditions, to a thin-branching shape in sheltered conditions (Kaandorp 1999). These morphologic modifications, resulting in changes to relative branch size, spacing, and branching pattern, can in turn alter the structure of flow itself, both around and through colonies (Chamberlain and Graus 1975; Sebens et al. 1997). Therefore, there is an apparent feedback between water flow patterns and coral morphology, which may not only play a critical role in coral survival, affecting colony overturning and breaking (Done 1982), but also have a sig-

nificant effect on nutrient uptake (Atkinson and Bilger 1992), gas exchange, and particle capture (Sebens et al. 1996; Helmuth et al. 1997).

Ultimately, the rates at which coral transfer nutrients, remove wastes, and exchange gas are controlled by the exchange processes occurring at the solid-water interface along the surfaces of the coral. Rates of mass transfer are directly related to levels of mixing and shear stress that develop in the boundary layer immediately adjacent to the coral colony (Shashar et al. 1996). Laboratory measurements for unidirectional flow conditions have shown that high rates of nutrient transfer over coral communities can occur, in part, due to their extreme roughness that imparts frictional drag on the flow, as well as enhances shear and mixing (Bilger and Atkinson 1992; Thomas and Atkinson 1997). Oscillatory flow, generated by surface waves, can play a key factor in generating even larger increases in nutrient transfer (Atkinson et al. 2001; Hearn et al. 2001). For example, Carpenter and Williams (1993) found that oscillatory flow enhanced photosynthesis of reef algal turf by 20% compared with unidirectional flow. Likewise, Falter et al. (2005) found an increase of 30–40% in mass transfer under oscillatory versus steady flow conditions for plaster forms placed in different reef habitats. Whereas these findings suggest that wave action increases mass transfer due to changes in boundary layer flow structure and turbulence, little is known about how variations in wave-dominated flow regimes affect mass transport rates in reefs, or how changes in morphology may act to alter these rates. The question then arises: *How does the characteristic morphology of a coral colony affect mass transfer under oscillatory versus steady flow regimes?*

We used laboratory studies to examine (1) the general character of flow within and around branched coral colonies, and (2) rates of mass transfer from within the branching

¹ Present address: Department of Integrative Biology, University of California, Berkeley, California 94720.

Acknowledgments

We thank Marlin Atkinson and Jim Falter at the Hawaii Institute of Marine Biology for supplying the *P. compressa* coral skeletons and Bob Brown for the design and construction of the resonant wavemaker. This research was partially funded through a Stanford Bio-X Interdisciplinary Initiatives Grant. M.A.R. was supported by a Stanford Graduate Fellowship, and J.V.S. was supported through the Research Experience for Undergraduates program of Stanford University.

structure of the colonies, for both unidirectional and wave influenced flows. Planar laser-induced fluorescence (PLIF) was used to visualize the large-scale flow characteristics, and the dissolution of gypsum was used as a proxy for mass transfer within the structure of three morphologically distinct branching coral species. Particular attention is paid to the rates of mass transfer *within* the branching structure of the coral since this region contains most living-tissue surface area available for mass transfer and where morphology is likely to play a major role in the physiological functions of the coral (Goldshmid et al. 2004).

Methods—Experiments were performed using the skeletal structure of three coral species: *Porites compressa*, *Stylophora pistillata*, and *Pocillopora verrucosa*. These corals were chosen because of their differing branching morphology as well as diversity of physical environments where they typically grow. *P. compressa* corals were collected along the reef flat in Kaneohe Bay, Hawaii, in a water depth of 1 m, where typical wave periods range between $T = 5$ and 10 s and peak oscillatory currents range from 8 to 11 cm s⁻¹ at the depth of the coral (Koehl and Hadfield 2004). The reefs found in Kaneohe Bay are typical of many lagoonal reefs, where breaking waves drive oscillating currents on the reef flat (Falter et al. 2004) and generate primarily unidirectional flow in channels and lagoons (Sebens and Done 1992; Andrefouet et al. 2001). *S. pistillata* and *P. verrucosa* corals were collected along a section of fringing reef in the Gulf of Aqaba, Red Sea over a range of water depths between 2 and 10 m. Mean currents at this reef site in Eilat, Israel, are typically between 5 and 10 cm s⁻¹, with weak wind generated wave motion in the shallows ($T = 2.5$ s), and no measurable oscillatory motion in the deeper areas. These two species of coral are very common in the coral reefs throughout the Red Sea (Loya and Slobodkin 1971). The branching of both species is much more sparse in spacing and thin in dimension than that of *P. compressa*. All three species are characterized by having low living-tissue biomass, and therefore using skeletons instead of live coral has a minimal effect on flow dynamics.

Four coral heads from each of the three species were used in the studies. *S. pistillata* had the thinnest diameter branch and sparsest branching structure, followed by *P. verrucosa*, and then *P. compressa*. Care was taken to choose coral heads with similar overall shape of height and diameter but also that spanned the typical range of morphology within each species. Images of six of the 12 coral colonies used in the experiments are shown in Fig. 1. For each species, measurements were made of the average colony height and diameter, as well as average branch diameter (d), spacing (S), and void ratio (VR), defined as (Lowe et al. 2005):

$$VR = \frac{S + d}{d} \quad (1)$$

This ratio gives an approximate measure of the “porosity” of the branched coral—i.e., the open volume relative to coral branch volume within the coral structure—which can be easily measured in situ with minimal disturbance to the living corals. Values are given in Table 1. To determine characteristic branch diameter, 20 branches were chosen at random

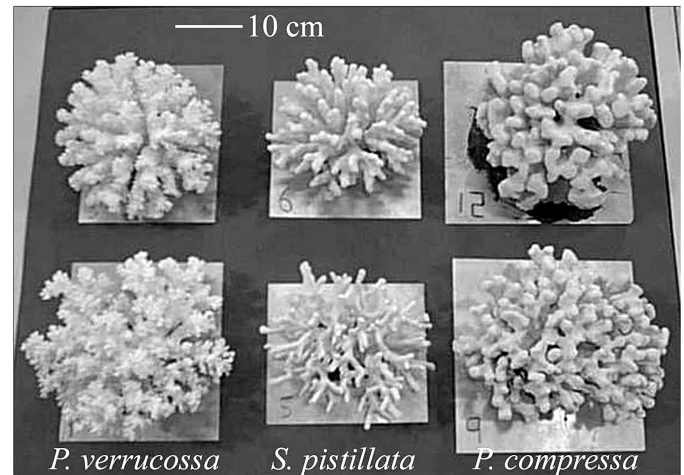


Fig. 1. Six of twelve coral colonies used in the experiments. Corals in each column are the same species, and from left to right are *Pocillopora verrucosa*, *Stylophora pistillata*, and *Porites compressa*.

on each coral and their diameters were measured using a digital caliper at 1 cm below the branch tip. To determine branch spacing, the average distance between nearest neighbor branches for 20 pairs of branches were measured along each coral, 1 cm below the branch tips. Within a given species, the void ratio varied by no more than 10% between different coral heads.

Planar laser-induced fluorescence (PLIF) was used to visualize the general flow characteristics around individual coral colonies. In this technique, 0.5 g L⁻¹ Rhodamine 6G dye was released to the interior of the coral through a 1 cm diameter tygon tube. Dye was injected at a rate of 3 mL min⁻¹ using a peristaltic pump, with a maximum linear velocity of 0.1 cm s⁻¹ to minimize momentum input from the injector. A 0.3-mm-thick laser-light sheet was created using a 514 nm laser (Coherent Innova model 90), focusing and collimating optics, and a scanning mirror (Cambridge Technology model 6800HP). As the light sheet passed over the imaging field, the dye fluoresced at a center wavelength of 555 nm. A light filter on the receiving optics removed the laser and ambient light, leaving only emitted light from the dye to be imaged using a CCD camera (Canon Elura MiniDV), which collected images at 30 frames per s.

The dissolution of gypsum (or gypsum-based plaster-of-Paris) was used as a relative measure of mass transfer and has been previously calibrated for many applications, especially in studies of physical-biological interactions (i.e., Sebens et al. 2003; Falter et al. 2005). Gypsum casts (commonly referred to as “clods”) were prepared with a mixture of 500 parts gypsum (CaSO₄ × H₂O C.A.S. 1010-14-4) to 335 parts water. Wet plaster was poured into 0.5 mL Eppendorph PCR tubes and a 15-cm-long, 0.1-mm steel wire was inserted through the clod while wet. Clods were allowed to dry for a minimum of 48 h and then removed from the Eppendorph containers and dried for an additional 4 days at ambient room temperature for complete drying. The dry weight of each clod was then measured before and after each

Table 1. Average dimensions of the coral colony height and diameter, branch spacing and diameter, and void ratio of the three coral species (± 1 standard deviation). Four coral heads were measured for each species. The branch diameter and spacing ($n=80$ measured per species) were used to calculate the void ratio (Eq. 1), with the standard deviation reported as the average variability within a colony.

| Coral type | Colony height (cm) | Colony diameter (cm) | Branch diameter (cm) | Branch spacing (cm) | Void ratio |
|----------------------|--------------------|----------------------|----------------------|---------------------|---------------|
| <i>S. pistillata</i> | 13 \pm 2 | 16 \pm 4 | 0.7 \pm 0.2 | 1.6 \pm 0.5 | 2.6 \pm 0.5 |
| <i>P. verrucosa</i> | 13 \pm 1 | 19 \pm 2 | 1.1 \pm 0.3 | 1.4 \pm 0.4 | 2.3 \pm 0.4 |
| <i>P. compressa</i> | 15 \pm 1 | 20 \pm 2 | 1.8 \pm 0.6 | 0.8 \pm 0.3 | 1.7 \pm 0.3 |

experiment using an analytical scale. The average dry weight of a clod was 8.3 \pm 0.5 g.

Five clods were suspended between the branches of each coral: one in the center and one each within the front, back, left, and right sides of the coral. Each clod was secured by wrapping the steel wire around a coral branch and was embedded approximately 5 cm below the top of the colony and a minimum of 3 cm from any outer edge of the colony. Care was taken to secure the clods so that they did not sway in the current. During each experiment, a “flow control” and “still control” was measured simultaneously. In the flow control, five clods were placed in the flume and exposed to free stream-flow conditions by attaching them to steel rods at heights that were comparable in height to those within the coral branches. In the still control, dissolution rates in no-flow conditions were measured by placing five gypsum clods, attached to steel rods, into a 20 L bucket filled with the same water as that in the flume. Weight loss of the clods was essentially linear with time until the gypsum dissolved to approximately 30% of original weight, similar to that found by Jokiel and Morrissey (1993). Each experiment was run between 5 and 10 h to achieve a sufficient dissolution signal but not allow nonlinearities in dissolution.

During the experiments, the 12 coral heads along with the flow control were placed in the flume and spaced sufficiently to minimize wake effects. For the still control, just before the start of each experiment, the 20 L container was filled with flume water to minimize temperature and ionic concentration differences. There was less than a 3% variance in the mean dissolution rate of the still control for all experiments, indicating that water temperature and chemistry variations were negligible between experiments. At least two experiments for each coral under each flow condition were run to give a minimum of 40 clod measurements per species per flow condition (i.e., 5 clods \times 4 specimens \times 2 replicates).

To carry out experiments over a broad range of unidirectional and wave-dominated flow regimes, two laboratory flume facilities were used, both capable of generating currents with or without waves. The first flume was a re-circulating flume that produced single frequency, progressive waves with periods up to 3 s. The flume dimensions were 12.5 m long by 1.20 m wide with a useable test section length of 7.3 m. Waves were generated using a paddle-type wavemaker, driven by a servo motor and linear actuator. A sloping broad-crested weir at the downstream end of the tank produced supercritical flow conditions at the weir and thereby minimized the reflection of wave energy. To generate a

longer wave with a period of 5 s, a second flume was used that had overall dimensions of 9 m long by 0.6 m wide, with a test section 5 m in length. The flume was fitted with a downstream plunger-type wavemaker that used the fundamental resonance of the tank to produce waves. The wavemaker oscillated a 10 cm diameter pvc tube in and out of the flow above the downstream flow-control weir of the tank. When the tube entered the flow, it prevented water from leaving the test section, thus setting up a wave that propagated upstream. The wave then reflected off the front of the flume and propagated back downstream. The wavemaker was run at a subharmonic resonance to magnify the amplitude of the wave. After a number of oscillations the amplitude of the wave grew sufficiently to allow the crest of the wave to spill over the top of the wavemaker tube, at which point the wave amplitude was held constant.

Coral skeletons containing gypsum clods were exposed to both unidirectional and wave-dominated flow conditions. Flow characteristics were measured using an Acoustic Doppler Velocimeter (Sontek Inc.) at a sampling rate of 25 Hz for 10 min. Velocities are reported in Table 2 as the mean free stream velocity (U_o), root mean-squared velocity (U_{rms}), wave orbital velocity amplitude (U_w), and the total velocity intensity (U_{total}), calculated as:

$$U_{total} = \frac{\sum_{i=1}^n |u_i| \Delta t}{T} \quad (2)$$

where u_i is the i^{th} measure of n instantaneous velocity measurements, Δt is the time duration of each measurement, and T is the total time interval of the measurements. U_{total} was used to represent total “water motion” because it integrates both steady flow as well as flow fluctuations (i.e., where wave velocities are both positive and negative) in a single measure. Equation 2 is written to point out that $|u_i| \Delta t$ is the distance over which a fluid parcel moves over the time period Δt , regardless of direction. It should be noted that for unidirectional flows, $U_o = U_{total}$, since flow reversal does not occur. For unidirectional flows, experiments were performed for four flow conditions of U_{total} : 2.9, 7.0, 10.8, and 14.1 cm s $^{-1}$. For the wave-dominated flows, experiments were performed at four flows that had wave periods of $T = 1, 2, 3,$ and 5 s. For all flow conditions, the mean water depth was 40 cm.

Results—A qualitative assessment of mass transport in steady and oscillatory flow was obtained by analyzing PLIF

Table 2. Unidirectional and wave-dominated flow conditions measured at 10 cm above the bed. U_{total} is the velocity defined in Eq. 2, U_o is the time-averaged velocity, U_{rms} is the root mean squared velocity, and U_w is the orbital wave velocity amplitude.

| | Wave period (s) | U_{total} (cm s ⁻¹) | U_o (cm s ⁻¹) | U_{rms} (cm s ⁻¹) | U_w (± cm s ⁻¹) |
|---------------------|-----------------|-----------------------------------|-----------------------------|---------------------------------|-------------------------------|
| Unidirectional flow | — | 2.9 | 2.9 | 3.0 | 0 |
| | — | 7.0 | 7.0 | 7.0 | 0 |
| | — | 10.8 | 10.8 | 10.8 | 0 |
| | — | 14.1 | 14.1 | 14.2 | 0 |
| Wave-dominated flow | 1 | 3.3 | 2.5 | 4.1 | 4.2 |
| | 2 | 5.2 | 2.8 | 6.0 | 7.7 |
| | 3 | 3.0 | 2.9 | 3.4 | 3.0 |
| | 5 | 7.9 | 5.3 | 8.6 | 9.0 |

images. Since the PLIF technique incorporates a continuous dye stream to the interior of the coral colony, variations in the *rates* of mass transfer could not be obtained, but changes in the *dynamics* of how mass is transferred could be visualized. Unidirectional and wave-dominated flow through a *S. pistillata* coral colony is shown in Fig. 2 (mean flow is from left to right), while video clips of the two flow conditions can be viewed in Web Appendix 1 at http://www.aslo.org/lo/toc/vol_51/issue_2/1134al.html. The waves shown ($T = 5$ s) were produced in a resonant wave flume where waves were traveling in both directions, therefore there is not a dominant direction of wave propagation.

For the unidirectional flow case (Fig. 2A), the flow is mostly diverted around the coral: flow near the top of the coral is pushed up and over the colony while water approaching the sides of the coral flows laterally around the coral. Water enters the interior of the coral along the upstream end and due to interaction with the coral branches, flow rates are quickly reduced and weak mixing and dispersal of the dye occurs. At the downstream end of the coral, a distinct wake region forms which contains a large, slowly circulating counter-clockwise eddy. This eddy formation is strongly characteristic of flow separation around the coral, and is bounded by a high shear region which forms at the top of the recirculation zone. This shear layer appears to be the location containing the most intense mixing and highest turbulent transport.

In comparison, the wave-dominated flow (Fig. 2B–D) shows a drastically different structure. As a result of the oscillatory motion there is no well-defined or persistent wake region on either side of the coral. Considerably more fluid appears to flow horizontally through the interior of the colony, while a significant amount of water is also dispersed upwards and out of the coral. Video clips of the flow field indicate that the dynamics of the fluid dispersal is timed with the oscillatory motion of the wave. As wave oscillations generate flow in the direction opposite of the mean current (from right to left in Fig. 2B), the fluid found along the downstream end of the coral accelerates upstream and is advected both through and around the coral. During peak flow reversal (Fig. 2C), negative horizontal velocities coincide with initial vertical motion that transports fluid away from the coral, while shear instabilities form on the upstream side of the coral, entraining dyed fluid from the coral interior. As flow reversal weakens, the vertical wave-induced flow transports

the entrained fluid upwards and away from the coral structure (Fig. 2D) before the oscillatory flow reverses again towards the same direction as the mean current. The general orbital motions of the water column follow what would be predicted from wave orbital theory. However, these flow visualizations indicate that wave-driven flow, interacting with the coral morphology, allows for substantially more water to penetrate to the interior of the coral compared to that of unidirectional flows, driving higher apparent rates of mass transport. Quantification of these relative rates of mass transport is obtained from measures of gypsum dissolution.

The dissolution rate of gypsum was measured as a percent dissolution per time, f_d :

$$f_d = \frac{W_i - W_f}{W_i \theta} \quad (3)$$

where W_i is the initial dry weight of the gypsum before the experiment, W_f is the dry weight at the end of the experiment, and θ is the duration, in hours, of the experiment. This formula gives the percent dissolution of gypsum per h ($\times 100\%$), and is a measure of the fractional amount of dissolved gypsum. Higher values of f_d correspond to greater dissolution, which in general results from an increase in water flux within the branching structure of the coral.

Dissolution rates as a function of velocity for both unidirectional and wave-dominated flow cases are shown in Fig. 3A. The free-stream values correspond to dissolution rates of the flow control. The difference in dissolution rates between the free stream and the coral is a reflection of the degree of “flow blockage” due to the coral branch structure. For the unidirectional flow cases, the trend is as expected: dissolution increases with increasing velocity and dissolution decreases with decreasing void ratio.

In Fig. 3B the dissolution values, normalized by the respective free-stream dissolution values of the flow control, are plotted as a function of flow velocity. The normalized dissolution values are a measure of the percent of gypsum dissolved within the coral relative to free stream conditions. Larger values (as one would expect for the *S. pistillata*, for example) indicate that relatively more flow passes through the coral structure. For unidirectional flows, normalized dissolution rates are relatively constant with respect to flow speed, signifying that the proportion of fluid moving through the coral relative to the external flow is roughly the same

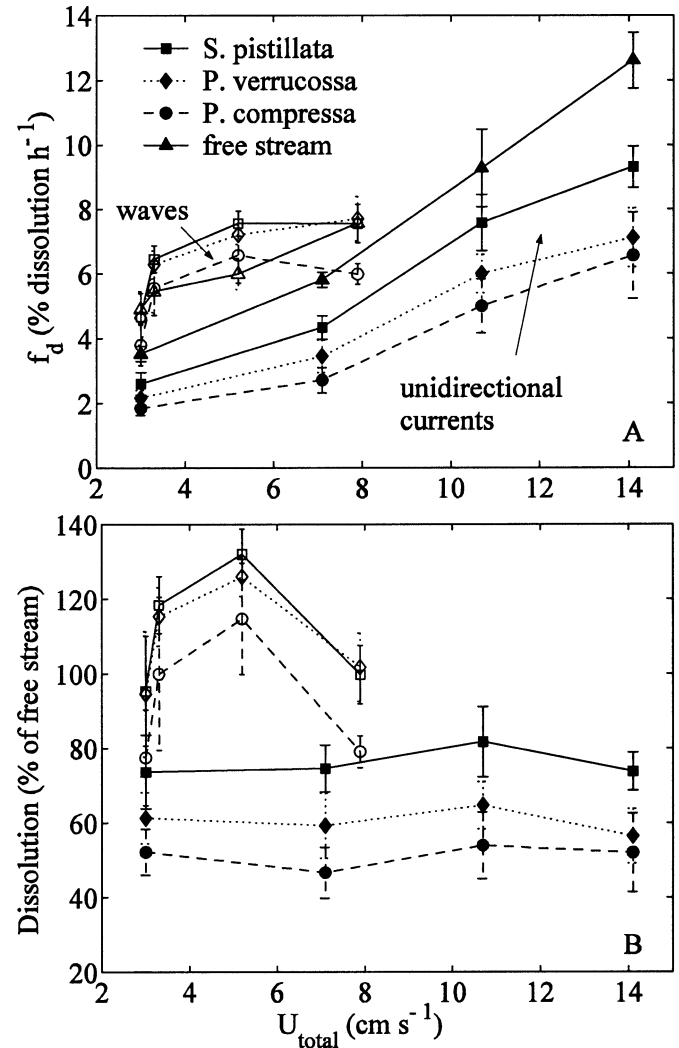
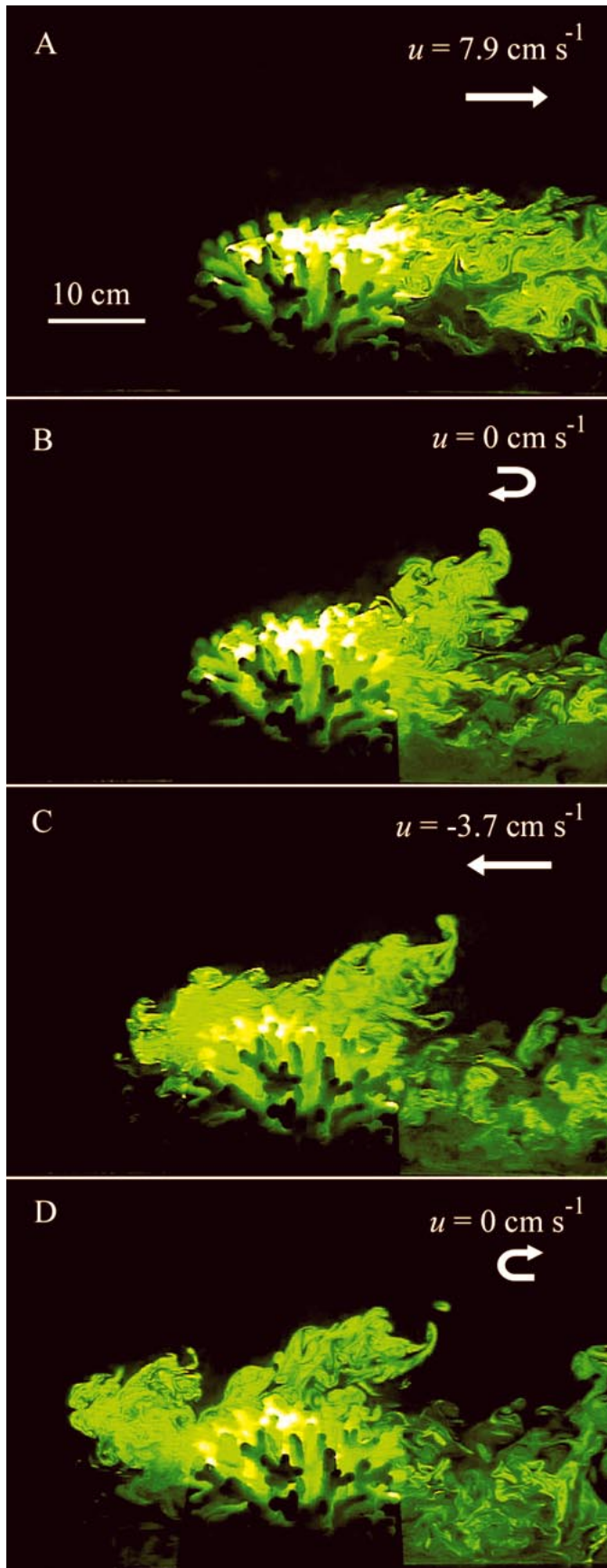


Fig. 3. (A) Percent dissolution of gypsum per time (as a percentage of initial weight) for unidirectional and wave-dominated flow conditions. Error bars are 95% confidence intervals. (B) Percent dissolution of gypsum within the branched coral structure relative to the dissolution rate of gypsum exposed to free stream conditions. A lower percentage means more flow is “blocked” by the coral structure. Solid symbols are unidirectional currents while open symbols are for wave-dominated currents.

←

Fig. 2. PLIF images of dye dispersal from the interior of a *Stylophora* coral during (A) unidirectional flow with $U_{total} = 7.9$ cm s⁻¹ and (B–D) oscillatory flow with a wave period of $T = 5$ s and $U_{total} = 7.9$ cm s⁻¹. Mean flow is from left to right with instantaneous velocities (u) reported on the images. The wave sequence is: (B) flow changing from forward to reverse direction (as compared to mean flow direction), (C) flow during reversal and (D) flow changing from reverse to forward direction.

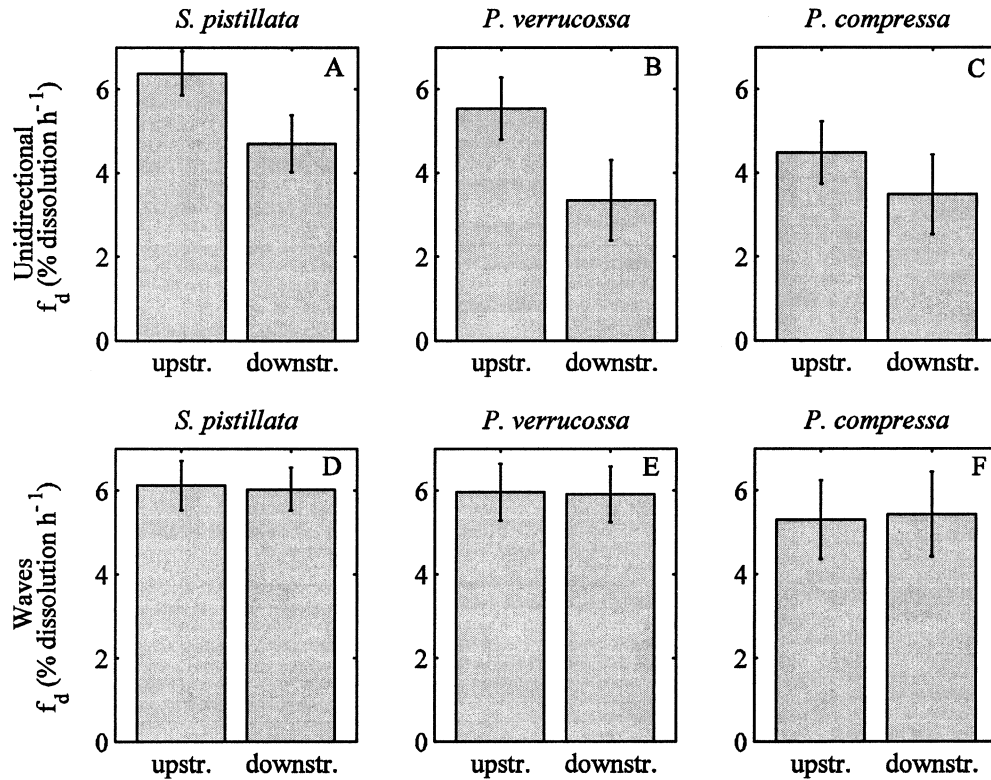


Fig. 4. Average percent dissolution of gypsum per time measured along the upstream and downstream sides within the coral for all the unidirectional (A–C) and oscillatory (D–F) flow conditions.

for all velocities measured. Mass transfer rates within the coral, compared to free stream values, are approximately 50%, 60%, and 75% for the *P. compressa*, *P. verrucosa*, and *S. pistillata* morphologies, respectively.

The results for the oscillatory flows (see Fig. 3A) indicate that waves greatly enhance mass transfer within the interior of the coral relative to unidirectional flows having the same total flow velocity. The general shape of the wave dissolution curves is also substantially different from those in unidirectional currents: dissolution no longer monotonically increases with flow velocity. As seen in Fig. 3B, when normalized by free-stream dissolution rates, the same dome shape is found for the wavy flows, unlike that for the unidirectional flows where the curve flattens. Noteworthy is the observation that in wave conditions of $U_{\text{total}} = 3.3$ and 5.2 cm s^{-1} , which correspond to oscillatory flows with the shortest wave periods measured of 1 and 2 s, respectively, the dissolution of gypsum is greater within the corals than in the free stream.

Locally within the coral, the net dissolution of gypsum clods placed along the upstream side of the coral was 29% greater than those placed along the downstream side under unidirectional flows, but there was only a 4% difference for wave conditions (Fig. 4). This variation suggests that in unidirectional currents, flow is attenuated as it passes through the coral, whereas under oscillatory flow, the attenuation is much less pronounced and a larger, more uniform within colony flow is generated.

Discussion—Wave action likely enhances mass transfer relative to steady currents by altering flow dynamics near the diffusing surface. The thickness of the diffusive boundary layer for concentration is a main determinant in the rate of mass transfer. This thickness is directly related to the momentum wave boundary layer thickness, l , which scales in oscillatory flow conditions as (Grant and Madsen 1979):

$$l = \kappa T \frac{U_*}{2\pi} \quad (4)$$

where κ is von Karman's constant = 0.41 and T is the wave period. This formulation shows that for a given shear velocity, a smaller wave period will result in a thinner wave boundary layer. Physically, this relationship occurs because, given similar wave friction velocities, a shorter wave period decreases the time available for a wave boundary layer to develop. Likewise, for similar values of wave orbital velocity, U_w , a shorter wave period should also increase the magnitude of water particle accelerations, increasing localized gradients in the flow.

To isolate the effect of wave period on dissolution rate and test the wave period scaling of Eq. 4 on mass transfer, dissolution rates for oscillatory flows ($f_{d,osc}$) can be normalized by dissolution rates for unidirectional flows ($f_{d,uni}$) under "equivalent" flow conditions: i.e., dissolution was estimated for unidirectional flows, using a spline curve fit, at values of U_{total} that matched the oscillatory conditions. These mass-transfer enhancement ratios, $E = f_{d,osc}/f_{d,uni}$, are shown in Ta-

Table 3. Enhancement ratio ($E = f_{d,osc}/f_{d,uni}$) of the dissolution of gypsum under waves vs. unidirectional velocities of the same U_{total} . Dissolution rates range between 1.6 to 2.9 times higher in wave-dominated compared to that of unidirectional currents, and increase with decreasing wave period, T .

| | $T=1$ s | $T=2$ s | $T=3$ s | $T=5$ s |
|----------------------|---------|---------|---------|---------|
| <i>S. pistillata</i> | 2.4±0.2 | 2.1±0.1 | 1.8±0.3 | 1.6±0.1 |
| <i>P. verrucosa</i> | 2.8±0.2 | 2.5±0.1 | 2.1±0.4 | 1.9±0.2 |
| <i>P. compressa</i> | 2.9±0.4 | 2.8±0.3 | 2.1±0.3 | 1.9±0.1 |
| Free stream | 1.4±0.2 | 1.3±0.1 | 1.4±0.1 | 1.4±0.1 |

ble 3 and indicate that the *relative* mass-transfer rates within the coral structure increase with decreasing wave period. As T decreases, higher ratios are also found for those corals with a smaller void ratio; i.e., the densely packed *P. compressa* coral has a greater relative mass-transfer rate under waves than *P. verrucosa*, or the most sparsely branched *S. pistillata* coral. Lowe et al. (2005) also found this same relationship in mass-transfer ratios for an idealized array of vertical cylinders, which was due to increased within-array flow speed ratios (between waves and steady currents) for tighter cylinder spacing. The trend of reduced relative mass-transfer rates with increasing wave period also indicates that rates will likely decrease to unidirectional mass-transfer rates as $T \rightarrow \infty$. Therefore, we would predict that for longer wave periods, the overall relative effect of wave action on mass transfer will be reduced.

For all the corals, the increase in relative mass transfer ranges between a factor of 1.6 for a $T = 5$ s wave period to 2.9 for a $T = 1$ s wave period. The increase for the free stream control under waves versus unidirectional currents was 1.3 to 1.4, though no statistical relation to wave period was found. This 30% to 40% increase in mass transfer under waves is the same as that found in field observations by Falter et al. (2005). Our finding of substantially higher mass-transfer ratios within the coral structure suggests that changes in local, wave-generated flow dynamics, interacting with the coral structure, allows for an increase in flux of water to the interior of the coral. Less flow is blocked by the coral branching structure in oscillatory flows and more uniform dissolution of gypsum occurs throughout a colony compared to unidirectional currents. In some instances, for flow conditions of $T = 1$ and 2 s in particular, mass transfer within the canopy was up to 130% of that compared to free stream conditions. One source for this increase may be due to the strong accelerations and decelerations in the flow that these short-period waves produce. Because the space between the coral branches can be considered “channels,” as flow is driven by large gradients in pressure between these channels, corresponding instantaneous fluid velocities and turbulence levels within the coral may achieve higher rates than those of free stream conditions.

Is the wave enhancement due to an increase in flow speed or turbulence within the coral? Although Falter et al. (2005) found wave enhancement primarily due to flow (acceleration) effects, they did note that dissolution of plaster forms was 20% greater with the addition of turbulence-generating coral rubble. Porter et al. (2000) also showed that changes

in the levels of turbulence could produce different mass-transfer rates without changes in bulk flow. This indicates that our measured increases can be due either to changes in flow or turbulence, but in all likelihood, is due to some combined effect of both. More detailed flow studies of direct velocity measurements within the branched corals are needed to confirm the dynamics, but the clear result is that mass transfer itself was greater, whatever the flow regime.

Since our gypsum dissolution experiments were conducted in an environment where rates were limited solely by the exchange across their diffusive boundary layer, these measurements only indicate potential rates of mass transfer within coral colonies; the actual rates in living reef systems may also depend on the kinetics of the exchange (Sanford and Crawford 2000) and behavior of the organism. However, Falter et al. (2004) has shown that nutrient uptake rates by reef flat communities exposed to wave action are occurring near maximal levels. Our results also agree with results by Atkinson et al. (2001) who measured increases in nutrient transfer of 2–3-fold when a living reef system was exposed to wave-dominated conditions, indicating that results presented in our study generally apply to entire reef environments that are under mass-transfer limitation.

In summary, rates of mass transfer in branched reef corals have been shown to be a function of both the physical flow environment and the morphology of their branching structure. Wave action, as well as unidirectional flow, both reduce the thickness of the boundary-layer flow around coral colonies and increases flow through the colony. Measured mass-transfer rates increased with increasing flow rate and void ratio. This suggests that in low-energy environments, a sparse branching structure of the coral morphology may be necessary to allow a sufficient flux of water to the interior of the colony. Yet, in wave-dominated flows, mass transfer was measured to be up to 3 times the rate for that of equivalent unidirectional currents. This may allow coral to effectively increase their branching density, thus increasing strength and surface area available for biomass growth, without adversely affecting the ability to uptake nutrients or undergo essential exchange processes.

References

- ANDREFOUET, S., J. PAGES, AND B. TARTINVILLE. 2001. Water renewal time for classification of atoll lagoons in the Tuamotu Archipelago (French Polynesia). *Coral Reefs* **20**: 399–408.
- ATKINSON, M. J., AND R. W. BILGER. 1992. Effects of water velocity on phosphate uptake in coral reef-flat communities. *Limnol. Oceanogr.* **37**: 273–279.
- , J. L. FALTER, AND C. J. HEARN. 2001. Nutrient dynamics in the Biosphere 2 coral reef mesocosm: water velocity controls NH_4 and PO_4 uptake. *Coral Reefs* **20**: 341–346.
- BILGER, R. W., AND M. J. ATKINSON. 1992. Anomalous mass transfer of phosphate on coral reef flats. *Limnol. Oceanogr.* **37**: 261–272.
- CARPENTER, R. C., AND S. L. WILLIAMS. 1993. Effects of algal turf canopy height and microscale substratum topography of profiles of flow speed in a coral forereef environment. *Limnol. Oceanogr.* **38**: 687–694.
- CHAMBERLAIN, J. A., AND R. R. GRAUS. 1975. Water flow and hydro-mechanical adaptations of branched reef corals. *B. Mar. Sci.* **25**: 112–125.

- DONE, T. J. 1982. Patterns and distribution of coral communities across the central Great Barrier Relief. *Coral Reefs* **1**: 95–107.
- FALTER, J. L., M. J. ATKINSON, AND M. A. MERRIFIELD. 2004. Mass-transfer limitation of nutrient uptake by a wave-dominated reef flat community. *Limnol. Oceanogr.* **49**: 1820–1831.
- , ———, AND C. F. M. COIMBRA. 2005. Effects of surface roughness and oscillatory flow on the dissolution of plaster forms: Evidence for nutrient mass transfer to coral reef communities. *Limnol. Oceanogr.* **50**: 246–254.
- GOLDSHMID, R., R. HOLZMAN, D. WEIHS, AND A. GENIN. 2004. Aeration of corals by sleep-swimming fish. *Limnol. Oceanogr.* **49**: 1832–1839.
- GRANT, W. D., AND O. S. MADSEN. 1979. Combined wave and current interaction with a rough bottom. *J. Geophys. Res.* **84**: 1797–1808.
- GRAUS, R. R., AND I. G. MACINTYRE. 1989. The zonation patterns of Caribbean coral reefs as controlled by wave and light energy input, bathymetric setting and reef morphology: computer simulation experiments. *Coral Reefs* **8**: 9–18.
- HAMNER, W., AND E. WOLANSKI. 1988. Hydrodynamic forcing functions and biological processes on coral reefs: A status review. *Proc. 6th Int. Coral Reef Symp.* **1**: 103–113.
- HEARN, C. J., M. J. ATKINSON, AND J. L. FALTER. 2001. A physical derivation of nutrient-uptake rates in coral reefs: effects of roughness and waves. *Coral Reefs* **20**: 347–356.
- HELMUTH, B. S. T., K. P. SEBENS, AND T. L. DANIEL. 1997. Morphological variation in coral aggregations: branch spacing and mass flux to coral tissues. *J. Exp. Mar. Biol. Ecol.* **209**: 233–259.
- JOKIEL, P. L., AND J. I. MORRISSEY. 1993. Water motion on coral reefs: evaluation of the ‘clod card’ technique. *Mar. Ecol. Prog. Ser.* **93**: 175–181.
- KAANDORP, J. A. 1999. Morphological analysis of growth forms of branching marine sessile organisms along environmental gradients. *Mar. Biol.* **134**: 295–306.
- KENCH, P. S. 1998. Physical processes in an Indian Ocean atoll. *Coral Reefs* **17**: 155–168.
- KOEHL, M. A. R., AND M. G. HADFIELD. 2004. Soluble settlement cue in slowly-moving water within coral reefs induces larval adhesion to surfaces. *J. Mar. Sys.* **49**: 75–88.
- LESSER, M. P., V. WEISS, M. R. PATTERSON, AND J. JOKIEL. 1994. Effects of morphology and water flow on carbon delivery and productivity in the Reef Coral, *Pocillopora damicornis*: Diffusion barriers, inorganic carbon limitation, and biochemical plasticity. *J. Exp. Mar. Biol. Ecol.* **178**: 153–179.
- LOWE, R. L., J. R. KOSEFF, S. G. MONISMITH, AND J. L. FALTER. 2005. Oscillatory flow through submerged canopies: 2. Canopy mass transfer. *J. Geophys. Res.* **110**: C10017, doi:10.1029/2004JC002789.
- LOYA, Y., AND L. B. SLOBODKIN. 1971. The coral reefs of Eilat (Gulf of Eilat, Red Sea). *Symp. Zoo. Soc. London* **28**: 117–139.
- PORTER, E. T., L. R. SANFORD, AND S. E. SUTTLES. 2000. Gypsum dissolution is not a universal integrator of ‘water motion’. *Limnol. Oceanogr.* **45**: 145–158.
- SANFORD, L. P., AND S. M. CRAWFORD. 2000. Mass transfer versus kinetic control of uptake across solid-water boundaries. *Limnol. Oceanogr.* **45**: 1180–1186.
- SEBENS, K. P., AND T. J. DONE. 1992. Water flow, growth form and distribution of scleractinian corals: Davies Reef, (GBR), Australia. *Proc. 7th Int. Coral Reef Symp.* **1**: 557–568.
- , K. S. VANDERSALL, L. A. SAVINA, AND K. R. GRAHAM. 1996. Zooplankton capture by two scleractinian corals, *Madracis mirabilis* and *Montastrea cavernosa*. *Mar. Biol.* **127**: 303–317.
- , J. WITTING, AND B. HELMUTH. 1997. Effects of water flow and branch spacing on particle capture by the reef coral *Madracis mirabilis* (Duchassaing and Michelotti). *J. Exp. Mar. Biol. Ecol.* **211**: 1–28.
- , B. S. T. HELMUTH, E. CARRINGTON, AND B. AGIUS. 2003. Effects of water flow on growth and energetics of the scleractinian coral *Agaricia tenuifolia* in Belize. *Coral Reefs* **22**: 35–47.
- SHASHAR, N., S. KINANE, P. L. JOKIEL, AND M. R. PATTERSON. 1996. Hydromechanical boundary layers over a coral reef. *J. Exp. Mar. Biol. Ecol.* **199**: 17–28.
- THOMAS, F. I. M., AND M. J. ATKINSON. 1997. Ammonium uptake by coral reefs: Effects of water velocity and surface roughness on mass transfer. *Limnol. Oceanogr.* **42**: 81–88.

Received: 7 June 2005

Accepted: 3 November 2005

Amended: 25 November 2005